Title

Diurnal Temperature and Pressure Effects on Axial Turbomachinery Stability in Solid Oxide Fuel Cell-Gas Turbine Hybrid Systems

Journal

JOURNAL OF FUEL CELL SCIENCE AND TECHNOLOGY, 8(3)

ISSN

1550-624X

Authors

Maclay, James D
Brouwer, Jacob
Samuelsen, G Scott

Publication Date

2011

DOI

10.1115/1.4003163

Diurnal Temperature and Pressure Effects on Axial Turbomachinery Stability in Solid Oxide Fuel Cell-Gas Turbine Hybrid Systems

James D. Maclay

Jacob Brouwer[1]
e-mail: jb@nfcrc.uci.edu

G. Scott Samuelsen

Advanced Power and Energy Program,
University of California, Irvine,
Irvine, CA 92697

A dynamic model of a 100 MW solid oxide fuel cell-gas turbine hybrid system has been developed and subjected to perturbations in diurnal ambient temperature and pressure as well as load sheds. The dynamic system responses monitored were the fuel cell electrolyte temperature, gas turbine shaft speed, turbine inlet temperature, and compressor surge. Using a control strategy that primarily focuses on holding fuel cell electrolyte temperature constant and secondarily on maintaining gas turbine shaft speed, safe operation was found to occur for expected ambient pressure variation ranges and for ambient temperature variations up to 28 K when tested nonsimultaneously. When ambient temperature and pressure were varied simultaneously, stable operation was found to occur when the two are in phase but not when the two are out of phase. The latter case leads to shaft overspeed. Compressor surge was found to be more likely when the system is subjected to a load shed initiated at minimum ambient temperature rather than at maximum ambient temperature. Fuel cell electrolyte temperature was found to be well-controlled except in the case of shaft overspeeds. Turbine inlet temperature remained in safe bounds for all cases. [DOI: 10.1115/1.4003163]

1 Introduction

The need for advanced coal based power generation has led to the concept of an integrated gasification fuel cell system (IGFC). The main power block in this system is composed of a solid oxide fuel cell (SOFC) integrated with a gas turbine (GT) operating on coal syngas. Detailed descriptions of such an integrated hybrid cycle or of a simple-cycle SOFC operating on coal syngas have been outlined in the literature [1–4]. The main benefits of IGFC systems are that they allow operation on an abundant and cheap fuel and by using syngas in place of solid coal, many of the toxic emissions associated with coal based power generation are removed. Additional benefits include very high electrical efficiencies that are possible by using a SOFC-GT hybrid system [5–14], and the separated anode and cathode flows of a fuel cell that more readily enable carbon concentration for sequestration. Finally, synergies between the SOFC and various gasifiers can be exploited to further increase overall system efficiency. One such potential synergy involves creating a higher methane content syngas, which improves the cold-gas efficiency of the gasifier. This is accomplished via internal reformation within the fuel cell, which provides a means of fuel cell cooling, reducing the excess air required for cooling and averting the associated parasitic losses.

In this study, a dynamic SIMULINK model of a 100 MW SOFC-GT operating on coal syngas is subjected to perturbations from steady state operation and the dynamic response is observed. The goals of this study are to establish and quantify the dynamic response of turbomachinery in hybrid SOFC-GT power blocks designed for use in IGFC applications and to delineate failure mechanisms and the means to mitigate failure mechanisms. The authors are unaware of any published research that characterizes the dynamic performance of turbomachinery applied to a SOFC-GT in an IGFC system. The model approach, developed by the National Fuel Cell Research Center (NFCRC) for these purposes, has been extensively peer-reviewed and validated using dynamic experimental data from a 220 kW Siemens–Westinghouse SOFC-GT system tested at the NFCRC [15–24].

2 Model and Operating Conditions

The SOFC-GT system model is diagrammed in Fig. 1. Coal syngas is fed to the fuel cell, while unutilized fuel is combusted and the hot gases are expanded through a turbine to power a generator and compressor that supplies air to the fuel cell. It is assumed that the fuel cell is designed in such a way as to preheat the incoming air and fuel. This strategy was employed in the Siemens–Westinghouse design referenced above and most other fuel cell system designs. Air preheating is principally accomplished using a cathode blower that recirculates hot cathode exhaust and mixes it with the air exiting the compressor.

The composition of the coal syngas is shown in Table 1. It is predominantly composed of hydrogen with only minor fractions of methane and carbon monoxide. The reason that the nitrogen, water, and carbon dioxide fractions are so low is that the cryogenic air separation, dehydration, and carbon dioxide removal steps, respectively, are carried out in the gasifier to enable carbon sequestration. A detailed model description of the gasifier and other cycle components is outside the scope of this paper, which focuses on the SOFC-GT power block. The gasifier concept, however, is also being developed by the Advanced Power and Energy Program (APEP) at the University of California, Irvine, based upon previous similar gasifier concepts found in Refs. [3], [12], and [25]. Because of the low hydrocarbon and carbon monoxide content relative to hydrogen, an external reformer is not required

[1]Corresponding author.

Contributed by the Advanced Energy Systems Division of ASME for Publication in the JOURNAL OF FUEL CELL SCIENCE AND TECHNOLOGY. Manuscript received September 27, 2010; Final manuscript received November 9, 2010; published online March 1, 2011. Editor: Nigel M. Sammes.

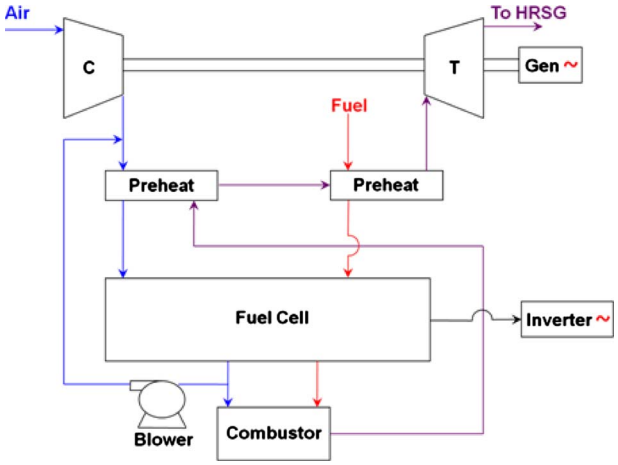

Fig. 1 SOFC-GT hybrid system utilizing a blower for cathode recirculation

in the current case. Internal reformation and water-gas-shift reaction chemistry is included in the model to account for conversion of all the nonhydrogen fuel constituents.

2.1 Overall SOFC-GT Model Formulation. The 100 MW SOFC-GT employs planar fuel cell geometry and empirical axial gas turbine compressor and turbine maps obtained from GSP [26]. Fuel cell operation is restricted to a fuel utilization at or below 80%. Steady state fuel cell operation is restricted to an average cell temperature of 1023 K+/−25 K, a maximum temperature rise across the cathode and anode of 150 K, and air preheat within the stack of 150 K. Steady state cycle pressure is 5 atm measured at the turbine inlet.

A detailed description of model development is presented in the literature [15–24]. Briefly, conservation of mass, energy, and momentum equations are solved for each major component within the model. The law of continuity is applied on a molar basis assuming a well-stirred reactor.

$$V_{cv}C\frac{d\mathbf{X}_{\text{out}}}{dt} = \dot{N}_{\text{in}}(\mathbf{X}_{\text{in}} - \mathbf{X}_{\text{out}}) - \mathbf{X}_{\text{out}}\sum \mathbf{R} + \mathbf{R} \tag{1}$$

where V_{cv} is the control volume (m^3), C is the molar concentration of the control volume (kmol/m^3), $\dot{N}_{\text{in}}$ is the molar flow rate into control volume (kmol/s), $\mathbf{X}_{\text{out}}$ is the mole fraction distribution vector out of the control volume, $\mathbf{X}_{\text{in}}$ is the mole fraction distribution vector entering the control volume, and $\mathbf{R}$ is the finite reaction rate vector (kmol/s).

The internal reformation model considers the chemical kinetics of steam reformation of methane and the water-gas shift reaction.

Conservation of energy for gaseous species is solved in each of the major components using

Table 1 SOFC-GT fuel stream specifications

Constituent	Mole fraction (%)
N_2	1.02
Ar	1.08
H_2	91
CO	2.62
CO_2	3.78
H_2O	0.01
CH_4	0.49
Total (%)	100

$$NC_v\frac{dT}{dt} = \dot{N}_{\text{in}}h_{\text{in}} - \dot{N}_{\text{out}}h_{\text{out}} + \sum \dot{Q}_{\text{in}} - \sum \dot{W}_{\text{out}} \tag{2}$$

where, N is the moles (kmol), $C_{v,\text{molar}}$ is the molar specific heat of the bulk mixture (J/kmol·K), T is the temperature of the bulk mixture (K), $\dot{N}_{\text{in}}$ is the molar flow rate into control volume (kmol/s), h_{in} is the sensible enthalpy into the control volume (J/kmol), $\dot{N}_{\text{out}}$ is the molar flow rate out of control volume (kmol/s), h_{out} is the sensible enthalpy out of the control volume (J/kmol), $\dot{Q}_{\text{in}}$ is the rate of heat energy flowing into the control volume (W), and $\dot{W}_{\text{out}}$ is the rate of work flowing out of the control volume (W).

Conservation of energy in the solid phase is solved where applicable using

$$\frac{d\rho C_{\text{mass}}TV_s}{dt} = \dot{E}_{\text{in}} - \dot{E}_{\text{out}} \tag{3}$$

where, C_{mass} is the specific heat of the solid (J/kg·K), T is the temperature of the solid (K), V_s is the volume of the solid (m^3), $\dot{E}_{\text{in}}$ is the rate of energy flowing into the solid (W), $\dot{E}_{\text{out}}$ rate of energy flowing out of the solid (W), and ρ is the density of the solid (kg/m^3).

Heat transfer is calculated in each layer of the cell, consisting of anode separator plate, anode fuel flow, anode, electrolyte, cathode, cathode air flow, and cathode separator plate, as well as for internal reformation. Heat transfer in the form of solid conduction, gases convection, sensible enthalpy of the gases, and a heat generation term are accounted for; radiation is neglected.

Applying Newton's Second Law on a fluid element the pressure loss is given by

$$P_{\text{in}} - P_{\text{out}} = \Delta P = f\frac{L}{D_h}\frac{\rho U^2}{2} \tag{4}$$

where, P_{in} is the pressure of the gas entering the control volume (Pa), P_{out} is the pressure of the gas leaving the control volume (Pa), ΔP is the pressure change of the gas through control volume (Pa), f is the friction factor through theory\experiment, L is the length of the fuel cell in the direction of flow (m), D_h is the hydraulic diameter of the channel (m), U is the bulk velocity of the fluid in the channel (m/s), and ρ is the density of the solid (kg/m^3). The flow inside the fuel cell is assumed to be a fully developed laminar flow.

Fuel cell voltage is calculated using the Nernst equation and activation; ohmic and concentration polarizations are accounted for.

The lumped parameter gas turbine model uses steady state gas turbine maps with dynamic mass storage and shaft speed equations.

2.2 Control. The system was found to require control for a stable and safe operation. The control strategy employed utilizes a cascade proportional-integral (PI) controller (Fig. 2). The controller provides stable SOFC temperature by using a variable speed gas turbine to deliver the proper air flow rate. This type of control was found to be necessary to avoid damaging fuel cell temperature excursions during dynamic response to system perturbations. Fuel cell electrolyte temperature is controlled to be constant at 1100 K while gas turbine shaft speed is secondarily controlled to remain close to the set-point value of 3600 rpm.

A cascade controller, very similar to that employed on the SOFC-GT, is used to control the blower/compressor mixture temperature at 800 K and to secondarily control blower speed. The blower is driven by an electrical motor. Due to the fuel cell control temperature of 1100 K, the blower is routinely operated near this temperature, which may not be practical using available technology.

The perturbation and dynamic response analysis consists of di-

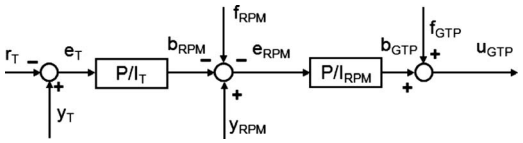

Fig. 2 Cascade controller used to control SOFC temperature with a variable speed gas turbine

urnal ambient temperature and pressure variations both separately and together. The diurnal temperature variation is also imposed for a case where the system is subjected to a 25% load shed.

The goal during the perturbation and dynamic response analysis is to maintain stable turbomachinery throughout as well as to maintain the SOFC control temperature of 1100 K. For safe turbomachinery operation compressor, surge and gas turbine shaft overspeed must be avoided; also, turbine inlet temperature (TIT) must remain below 1123 K.

3 Results and Discussion

3.1 Diurnal Ambient Temperature Fluctuations. When the hybrid system is subjected to a diurnal sinusoidal oscillation in an ambient temperature of 298 K+/−14 K (Fig. 3), the compressor remains in a stable region of operation. As ambient temperature rises, shaft speed increases in an effort to maintain the set-point temperature of 1100 K. This pushes compressor operation away from the surge line. However, as ambient temperature drops, the opposite is true and the compressor approaches the surge line.

When ambient temperature oscillates from 284K to 312 K (Fig. 4), the gas turbine shaft speed oscillates from 3475 rpm to 3745 rpm.

When ambient temperature oscillates from 284 K to 312 K (Fig. 5), turbine inlet temperature oscillates from 1004 K to 1012 K and fuel cell electrolyte temperature remains constant at 1110 K. The results for the case of a diurnal sinusoidal oscillation in an ambient temperature of 298 K+/−14 K show turbomachinery operation within safe boundaries but with a reduction in the surge margin that occurs in the trough of ambient temperature.

When the hybrid system is subjected to a diurnal sinusoidal oscillation in an ambient temperature of 298 K+/−16 K (Fig. 6), the compressor overspeeds in an effort to maintain the fuel cell set-point temperature during the initial rise in ambient temperature. The magnitude of diurnal temperature oscillation here may occur in many regions (especially deserts) and, as a result, must be considered during design to ensure stable and safe operation. Compressor overspeed in this case is considered a turbomachinery failure.

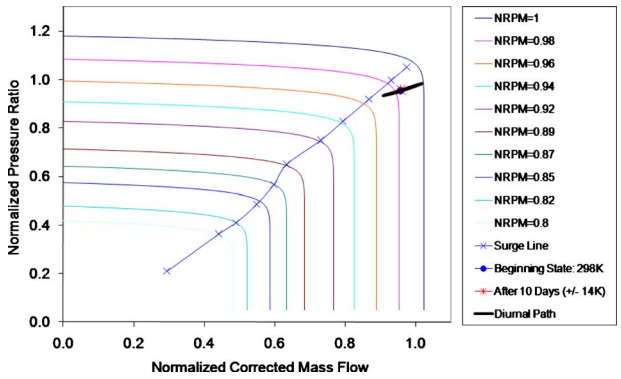

Fig. 3 Compressor response to a diurnal temperature fluctuation of 28 K

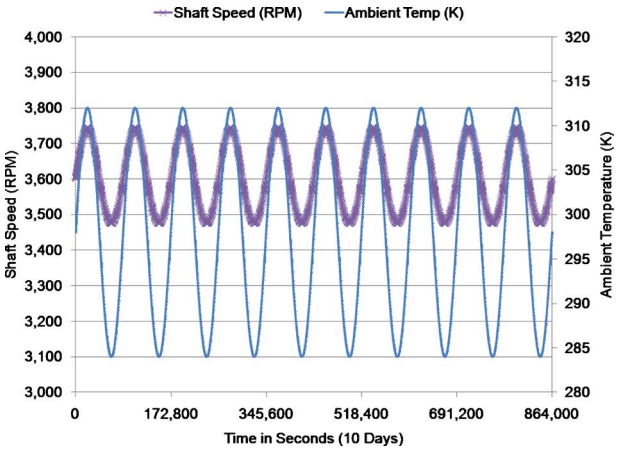

Fig. 4 Ambient temperature and gas turbine shaft speed versus time for a diurnal temperature fluctuation of 28 K

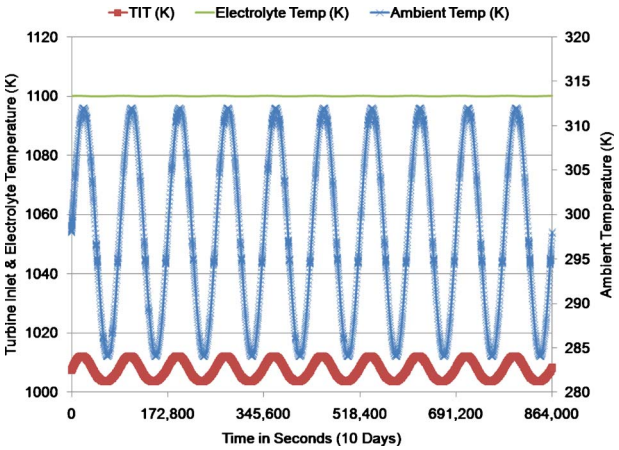

Fig. 5 Ambient temperature, turbine inlet temperature, and fuel cell electrolyte temperature versus time for a diurnal temperature fluctuation of 28 K

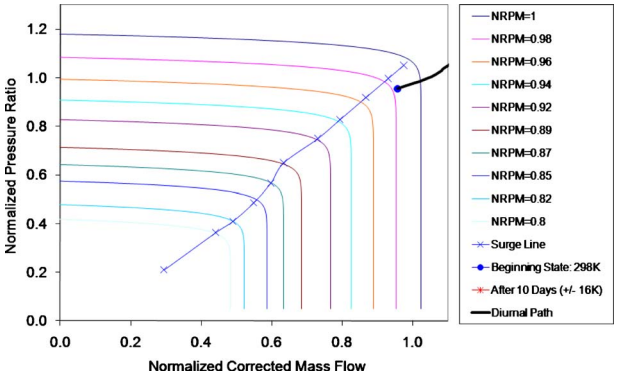

Fig. 6 Compressor response to a diurnal temperature fluctuation of 32 K

3.2 Diurnal Ambient Temperature Fluctuations (Fuel Cell Subjected to a 25% Decrease in Current Demand). When the hybrid system is subjected to a 25% decrease in fuel cell current demand (Fig. 7), compressor surge is approached at the minimum load value.

When the hybrid system is subjected to perturbations of a diurnal sinusoidal oscillation in an ambient temperature of 298 K+/

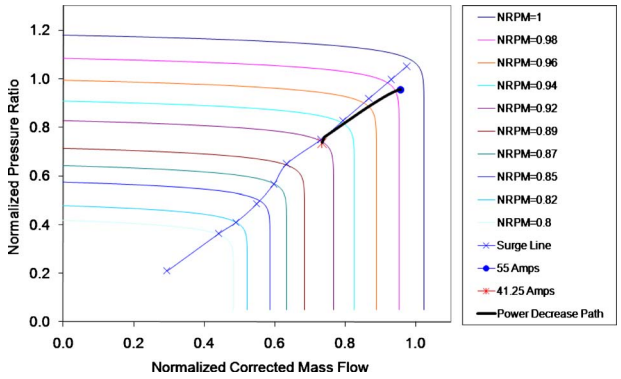

Fig. 7 Compressor response to a 25% reduction in fuel cell current demand

−14 K (Fig. 8) and a 25% reduction in fuel cell current initiated at the minimum ambient temperature, the compressor crosses the surge line almost immediately. This is a result of operating the compressor near the surge line at minimum ambient temperature, the point of minimum mass flow, and rpm requirement for the controlled fuel cell set-point temperature of 1100 K. Compressor surge in this case is considered a failure.

When the hybrid system is subjected to a diurnal sinusoidal oscillation in an ambient temperature of 298 K+/−14 K (Fig. 9) and a 25% reduction in fuel cell current demand is initiated at the maximum ambient temperature, the compressor crosses the surge line only once the minimum load is reached. Surge is initially avoided due to compressor operation far from the surge line at

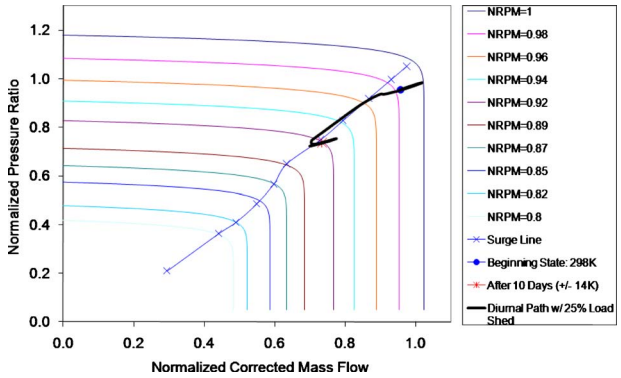

Fig. 8 Compressor response to a diurnal temperature fluctuation of 28 K and a 25% reduction in fuel cell current demand initiated at minimum ambient temperature

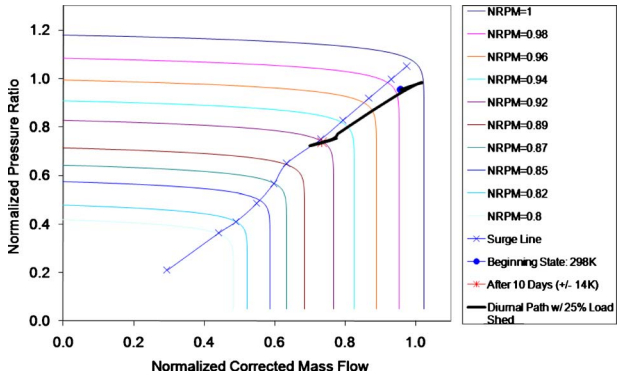

Fig. 9 Compressor response to a diurnal temperature fluctuation of 28 K and a 25% reduction in fuel cell current demand initiated at maximum ambient temperature

maximum ambient temperature, the point of maximum mass flow, and RPM requirement for the controlled fuel cell set-point temperature of 1100 K. Compressor surge in this case is considered a failure.

3.3 Diurnal Ambient Pressure Fluctuations. When the hybrid system is subjected to a diurnal sinusoidal oscillation in an ambient pressure of 101.3 kPa+/−2 kPa (Fig. 10), the compressor remains in a stable region of operation. Ambient pressure oscillations exceeding +/−2 kPa are unlikely to occur. When ambient pressure reaches a minimum, gas turbine shaft speed reaches a maximum as it is more difficult to cool the fuel cell with a less dense fluid. The converse is true as ambient pressure reaches a maximum.

When ambient pressure oscillates from 99.3 kPa to 103.3 kPa (Fig. 11), gas turbine shaft speed oscillates from 3579 rpm to 3626 rpm.

When ambient pressure oscillates from 99.3 kPa to 103.3 kPa (Fig. 12), turbine inlet temperature oscillates from 1007 K to 1008 K and fuel cell electrolyte temperature remains constant at 1110 K. The results for the case of a diurnal sinusoidal oscillation in an ambient pressure of 101.3 kPa+/−2 kPa show turbomachinery operation within safe boundaries.

3.4 Simultaneous Diurnal Ambient Temperature and Pressure Fluctuations. When the hybrid system is subjected to a simultaneous, in phase, diurnal sinusoidal oscillation in an ambient temperature of 298 K+/−14 K and an ambient pressure of 101.3 kPa+/−2 kPa (Fig. 13), the compressor remains in a stable region of operation. When compared with the case where

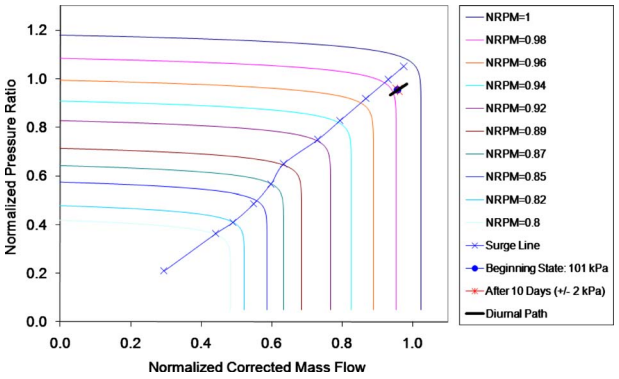

Fig. 10 Compressor response to a diurnal pressure fluctuation of 4 kPa

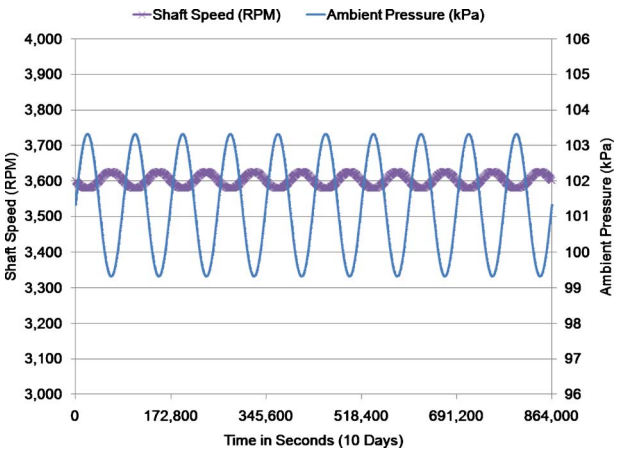

Fig. 11 Ambient pressure and gas turbine shaft speed versus time for a diurnal pressure fluctuation of 4 kPa

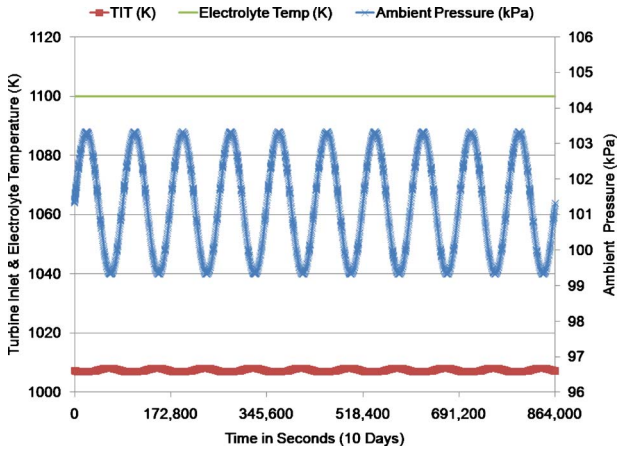

Fig. 12 Ambient pressure, turbine inlet temperature, and fuel cell electrolyte temperature versus time for a diurnal pressure fluctuation of 4 kPa

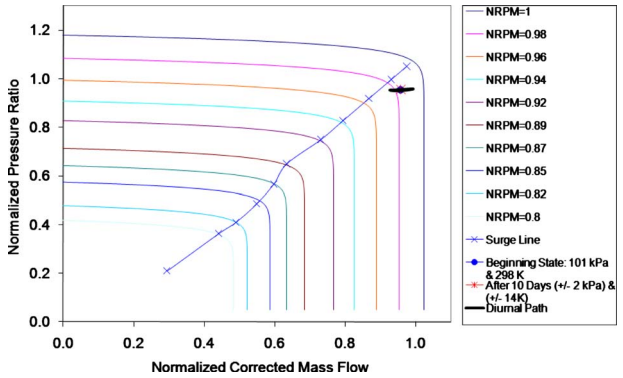

Fig. 13 Compressor response to a diurnal temperature fluctuation of 28 K and pressure fluctuation of 4 kPa in phase with each other

only ambient temperature is varied by 28 K (Fig. 3) or only ambient pressure is varied by 4 kPa (Fig. 10), the simultaneous, in phase variation damps the oscillation so that surge is less of a possibility.

When ambient temperature oscillates from 284 K to 312 K simultaneously in phase with ambient pressure oscillating from 99.3 kPa to 103.3 kPa (Fig. 14), the gas turbine shaft speed oscillates from 3494 rpm to 3718 rpm.

When ambient temperature oscillates from 284 K to 312 K simultaneously in phase with ambient pressure oscillating from 99.3 kPa to 103.3 kPa (Fig. 15), the turbine inlet temperature oscillates from 1004 K to 1011 K and the fuel cell electrolyte temperature remains constant at 1110 K. The results for the case of a diurnal sinusoidal oscillation in an ambient temperature of 298 K+/−14 K and in an ambient pressure of 101.3 kPa+/−2 kPa in phase show turbomachinery operation within safe boundaries.

When the hybrid system is subjected to a simultaneous, out of phase, diurnal sinusoidal oscillation in an ambient temperature of 298 K+/−14 K and an ambient pressure of 101.3 kPa+/−2 kPa (Fig. 16), the compressor overspeeds. When compared with the case where only ambient temperature is varied by 28 K (Fig. 3) or only ambient pressure is varied by 4 kPa (Fig. 10), the simultaneous, out of phase variation boosts the oscillation to a maximum rpm leading to overspeed. Compressor overspeed in this case is considered a failure.

The question arises as to whether ambient temperature and

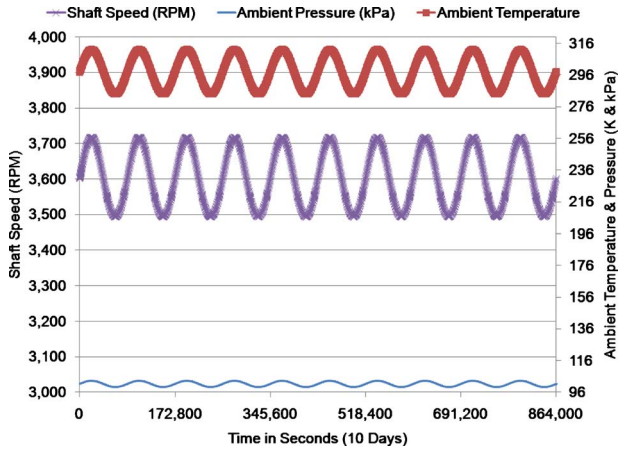

Fig. 14 Ambient temperature, ambient pressure, and gas turbine shaft speed versus time for a diurnal temperature fluctuation of 28 K and pressure fluctuation of 4 kPa in phase with each other

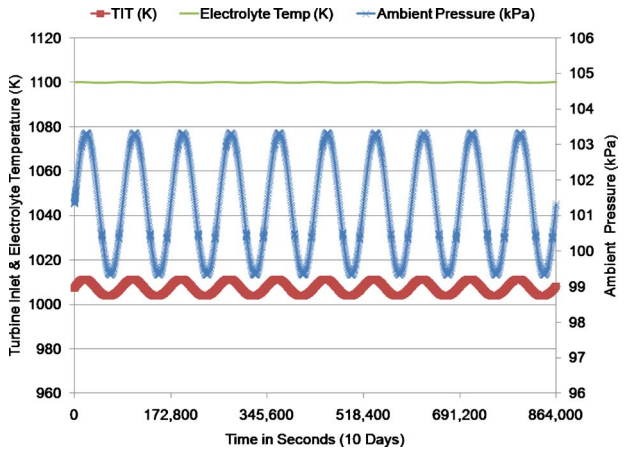

Fig. 15 Ambient pressure, turbine inlet temperature, and fuel cell electrolyte temperature versus time for a diurnal temperature fluctuation of 28 K and pressure fluctuation of 4 kPa in phase with each other

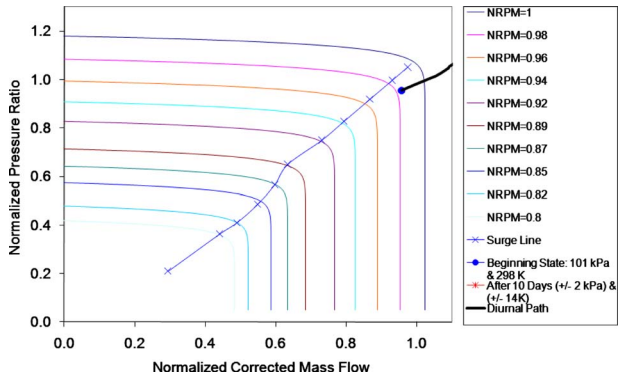

Fig. 16 Compressor response to a diurnal temperature fluctuation of 28 K and pressure fluctuation of 4 kPa out of phase with each other

pressure occur in or out of phase in the atmosphere. Plotting the data obtained from an atmospheric monitoring station located at Argonne National Laboratory [27] shows that either relationship is possible, as seen in Figs. 17 and 18.

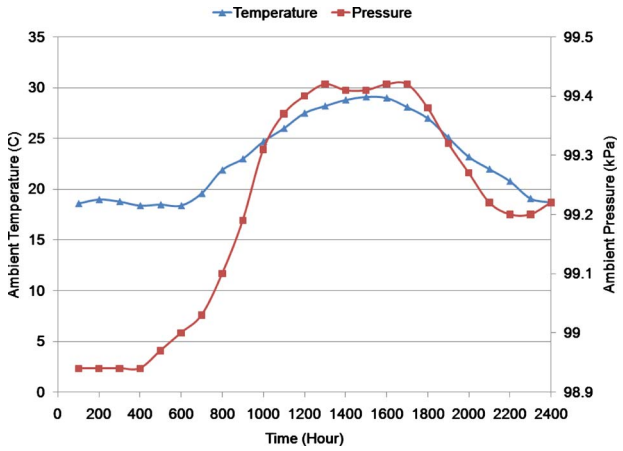

Fig. 17 Hourly ambient temperature and ambient pressure versus time for September 1, 2005. Source: Argonne National Laboratory.

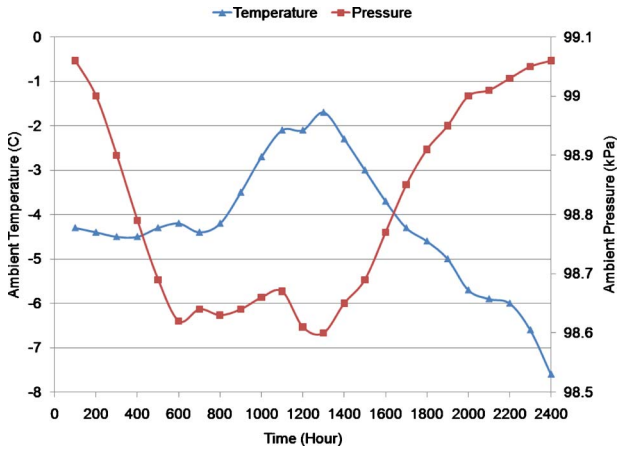

Fig. 18 Hourly ambient temperature and ambient pressure versus time for December 1, 2005. Source: Argonne National Laboratory.

4 Conclusions

A dynamic model of a 100 MW SOFC-GT hybrid system has been developed and subjected to perturbations in diurnal ambient temperature and pressure as well as load sheds. The dynamic system responses monitored were fuel cell electrolyte temperature, gas turbine shaft speed, turbine inlet temperature, and compressor surge. The hybrid system was found to operate within stable bounds for all cases tested except for excessive ambient temperature swings, simultaneous ambient temperature, and pressure variations that are out of phase and load sheds, especially those that occur in the presence of ambient temperature variations. The diurnal temperature ranges that led to system failures are likely to occur in many applications and need, as a result, to be considered in the design of turbomachinery and control systems for hybrid SOFC-GT systems. Special care should also be taken to minimize the impact of simultaneous environmental variations that may, by themselves, not be a concern. The confounding perturbations of environmental condition variations, such as ambient temperature variation, with operational condition variations, such as a load shed, were found to significantly impact operational stability.

Acknowledgment

The authors gratefully acknowledge the funding support of the U.S. Department of Energy (DOE) under Contract No. DE-AC26-04NT41817.313.01.05.036. We especially acknowledge the support and guidance of the program managers Wayne Surdoval and Travis Shultz.

References

[1] Jansen, D., van der Laag, P. C., Oudhuid, A. B. J., and Ribberink, J. S., 1994, "Prospects for Advanced Coal-Fuelled Fuel Cell Power Plants," J. Power Sources, **49**, pp. 151–165.
[2] Kuchonthara, P., Bhattacharya, S., and Tsutsumi, A., 2005, "Combination of Thermochemical Recuperative Coal Gasification Cycle and Fuel Cell for Power Generation," Fuel, **84**, pp. 1019–1021.
[3] Verma, A., Rao, A. D., and Samuelsen, G. S., 2006, "Sensitivity Analysis of a Vision 21 Coal Based Zero Emission Power Plant," J. Power Sources, **158**, pp. 417–427.
[4] Lobachyov, K., and Richter, H. J., 1996, "Combined Cycle Gas Turbine Power Plant With Coal Gasification and Solid Oxide Fuel Cell," ASME J. Energy Resour. Technol., **118**, pp. 285–292.
[5] Winkler, W., and Lorenz, H., 2002, "The Design of Stationary and Mobile Solid Oxide Fuel Cell-Gas Turbine Systems," J. Power Sources, **105**, pp. 222–227.
[6] Winkler, W., 2006, "Fuel Cell Hybrids, Their Thermodynamics and Sustainable Development," ASME J. Fuel Cell Sci. Technol., **3**, pp. 195–201.
[7] Winkler, W., Nehter, P., Williams, M. C., Tucker, D., and Gemmen, R., 2006, "General Fuel Cell Hybrid Synergies and Hybrid System Testing Status," J. Power Sources, **159**, pp. 656–666.
[8] Kurz, R., 2005, "Parameter Optimization on Combined Gas Turbine-Fuel Cell Power Plants," ASME J. Fuel Cell Sci. Technol., **2**, pp. 268–273.
[9] Park, S. K., Oh, K. S., and Kim, T. S., 2007, "Analysis of the Design of a Pressurized SOFC Hybrid System Using a Fixed Gas Turbine Design," J. Power Sources, **170**, pp. 130–139.
[10] Stiller, C., Thorud, B., Seljebo, S., Mathisen, O., Karoliussen, H., and Bolland, O., 2005, "Finite-Volume Modeling and Hybrid-Cycle Performance of Planar and Tubular Solid Oxide Fuel Cells," J. Power Sources, **141**, pp. 227–240.
[11] Rao, A. D., and Samuelsen, G. S., 2002, "Analysis Strategies for Tubular Solid Oxide Fuel Cell Based Hybrid Systems," ASME J. Eng. Gas Turbines Power, **124**, pp. 503–509.
[12] Rao, A. D., and Samuelsen, G. S., 2003, "A Thermodynamic Analysis of Tubular Solid Oxide Fuel Cell Based Hybrid Systems," ASME J. Eng. Gas Turbines Power, **125**, pp. 59–66.
[13] Magistri, L., Bozzolo, M., Tarnowski, O., Agnew, G., and Massardo, A. F., 2007, "Design and Off-Design Analysis of a MW Hybrid System Based on Rolls-Royce Integrated Planar Solid Oxide Fuel Cells," ASME J. Eng. Gas Turbines Power, **129**, pp. 792–797.
[14] Costamagna, P., Magistri, L., and Massardo, A. F., 2001, "Design and Part-Load Performance of a Hybrid System Based on a Solid Oxide Fuel Cell Reactor and a Micro Gas Turbine," J. Power Sources, **96**, pp. 352–368.
[15] Roberts, R. A., and Brouwer, J., 2006, "Dynamic Simulation of a 220 kW Solid Oxide Fuel-Cell-Gas-Turbine Hybrid System: Modeled Performance Compared to Measured Results," ASME J. Fuel Cell Sci. Technol., **3**, pp. 18–25.
[16] Roberts, R. A., Brouwer, J., Junker, T., and Ghezel-Ayagh, H., 2006, "Control Design of an Atmospheric Solid Oxide Fuel Cell/Gas Turbine Hybrid System: Variable Versus Fixed Speed Gas Turbine Operation," J. Power Sources, **161**, pp. 484–491.
[17] Roberts, R., Brouwer, J., Liese, E., and Gemmen, R. S., 2006, "Dynamic Simulation of Carbonate Fuel Cell-Gas Turbine Hybrid Systems," ASME J. Eng. Gas Turbines Power, **128**, pp. 294–301.
[18] Mueller, F., Brouwer, J., Jabbari, F., and Samuelsen, S., 2006, "Dynamic Simulation of an Integrated Solid Oxide Fuel Cell System Including Current-Based Fuel Flow Control," ASME J. Fuel Cell Sci. Technol., **3**, pp. 144–154.
[19] Kaneko, T., Brouwer, J., and Samuelsen, G. S., 2006, "Power and Temperature Control of Fluctuating Biomass Gas Fueled Solid Oxide Fuel Cell and Micro Gas Turbine Hybrid System," J. Power Sources, **160**, pp. 316–325.
[20] Mueller, F., Jabbari, F., Brouwer, J., Roberts, R., Junker, T., and Ghezel-Ayagh, H., 2007, "Control Design for a Bottoming Solid Oxide Fuel Cell Gas Turbine Hybrid System," ASME J. Fuel Cell Sci. Technol., **4**, pp. 221–230.
[21] Traverso, A., Massardo, A., Roberts, R. A., Brouwer, J., and Samuelsen, S., 2007, "Gas Turbine Assessment for Air Management of Pressurized SOFC/GT Hybrid Systems," ASME J. Fuel Cell Sci. Technol., **4**, pp. 373–383.
[22] Mueller, F., Jabbari, F., Gaynor, R., and Brouwer, J., 2007, "Novel Solid Oxide Fuel Cell System Controller for Rapid Load Following," J. Power Sources, **172**, pp. 308–323.
[23] Mueller, F., Brouwer, J., Kang, S., Kim, H. S., and Min, K., 2007, "Quasi-Three Dimensional Dynamic Model of a Proton Exchange Membrane Fuel Cell for System and Controls Development," J. Power Sources, **163**, pp. 814–829.
[24] Mueller, F., Gaynor, R., Auld, A. E., Brouwer, J., Jabbari, F., and Samuelsen, G. S., 2008, "Synergistic Integration of a Gas Turbine and Solid Oxide Fuel Cell for Improved Transient Capability," J. Power Sources, **176**, pp. 229–239.
[25] Yi, Y., Rao, A. D., Brouwer, J., and Samuelsen, G. S., 2004, "Analysis and Optimization of a Solid Oxide Fuel Cell and Intercooled Gas Turbine (SOFC–ICGT) Hybrid Cycle," J. Power Sources, **132**, pp. 77–85.
[26] Gas Turbine Simulation Program (GSP), http://www.gspteam.com/main/main.shtml
[27] Argonne National Laboratory, 2005, http://www.atmos.anl.gov/ANLMET/text/2005/